



Monitoring cell culture media degradation using surface enhanced Raman scattering (SERS) spectroscopy

Title	Monitoring cell culture media degradation using surface enhanced Raman scattering (SERS) spectroscopy
Author(s)	Calvet, Amandine;Ryder, Alan G.
Publication Date	2014-06-13
Publisher	Elsevier (Science Direct)
Repository DOI	10.1016/j.aca.2014.06.021

1 **Monitoring Cell Culture Media Degradation using Surface** 2 **Enhanced Raman Scattering (SERS) Spectroscopy.**

3
4 Amandine Calvet and Alan G. Ryder. *

5 Nanoscale Biophotonics Laboratory, School of Chemistry, National University of Ireland,
6 Galway, Galway, Ireland

7 * Corresponding author: **Email:** alan.ryder@nuigalway.ie **Phone:** +353-91-492943.

8 **Postal address:** Nanoscale Biophotonics Laboratory, School of Chemistry, National
9 University of Ireland, Galway, University Road, Galway, Ireland.

10
11 **Note:** This is the author version of the paper, the final published version DOI is:
12 [10.1016/j.aca.2014.06.021](https://doi.org/10.1016/j.aca.2014.06.021)

13 14 15 **Abstract:**

16 The quality of the cell culture media used in biopharmaceutical manufacturing is a crucial
17 factor affecting bioprocess performance and the quality of the final product. Due to their
18 complex composition these media are inherently unstable, and significant compositional
19 variations can occur particularly when in the prepared liquid state. For example photo-
20 degradation of cell culture media can have adverse effects on cell viability and thus process
21 performance. There is thus, from quality control, quality assurance and process management
22 view points, an urgent demand for the development of rapid and inexpensive tools for the
23 stability monitoring of these complex mixtures. Spectroscopic methods, based on
24 fluorescence or Raman measurements, have now become viable alternatives to more time-
25 consuming and expensive (on a unit analysis cost) chromatographic and/or mass
26 spectrometry based methods for routine analysis of media. Here we demonstrate the
27 application of Surface Enhanced Raman Scattering (SERS) spectroscopy for the simple, fast,
28 analysis of cell culture media degradation. Once stringent reproducibility controls are
29 implemented, chemometric data analysis methods can then be used to rapidly monitor the
30 compositional changes in chemically defined media. SERS shows clearly that even when
31 media are stored at low temperature (2-8 °C) and in the dark, significant chemical changes
32 occur, particularly with regard to cysteine/cystine concentration.

33
34 **Keywords:** Raman spectroscopy, Surface Enhanced Raman Scattering (SERS),
35 Biotechnology, cell culture media, photo-degradation, chemometrics.

36 37 38 **1. Introduction**

39 Cell culture media are an essential part of industrial mammalian cell culture,
40 sustaining optimal cell growth and ensuring correct product formation. In many cases
41 chemically defined (CD) media are now being used to avoid inconsistency issues associated
42 with complex hydrolysates and other biologically derived media. CD media are usually
43 complex aqueous chemical mixtures containing a range of amino acids, carbohydrates,
Page 1 of 19

44 vitamins, inorganic salts and other supplements. One such example is eRDF, an enriched
45 basal RDF medium containing higher amino acids and glucose concentrations which has ~60
46 components [1]. Media quality is absolutely critical to process performance, reliability, and
47 reproducibility. However, it is known that media are not chemically stable [2] and undergo
48 some slow rate chemical reactions when stored in the dark between 2-8 °C, the industry norm
49 for storing liquid cell culture media. It is also well known that chemical changes induced by
50 light exposure can adversely affect process performances and cell viability [2-8]. In addition,
51 some unstable components like cysteine are of particular interest since it and its oxidation
52 product, cystine, can have significant effects on protein aggregation [9]. Therefore it is
53 critical importance to assess and monitor media stability particularly during process
54 development where unknown/uncontrolled media variability can have very adverse
55 consequences. Multi-dimensional fluorescence in combination with chemometric data
56 analysis has been used to easily monitor light induced changes in media like eRDF [10, 11].
57 This was possible due to the fact that riboflavin and some of the significant photoactive
58 compounds (Tryptophan / Tyrosine) in the media are fluorescent. Furthermore, several
59 photoproducts were also fluorescent and so by use of chemometric tools like PARAFAC [12]
60 and MCR [13] it was possible to track composition changes. However this technique was not
61 able to detect changes affecting non-fluorescent original components or degradation products.

62 The use of Raman spectroscopy for media analysis can lead to a more comprehensive
63 analysis of the media composition because nearly all molecular constituents of media have
64 distinct Raman spectra and can easily be distinguished [14, 15]. Unfortunately, conventional
65 Raman spectroscopy is not good for analytes present in low concentration (<~0.5% w/w)
66 which is the case in most components in liquid cell culture media. One way in which
67 sensitivity can be enhanced is to use Surface Enhanced Raman Scattering (SERS) [16-18].
68 SERS is the enhancement effect on Raman scattering observed when molecules are adsorbed
69 onto nanosized noble metal structures, typically fabricated from gold or silver. SERS is
70 potentially a very sensitive analytical method (down to single molecule) for complex
71 biogenic materials analysis [16, 19, 20]. SERS measurements could provide valuable
72 information about variances in media in terms of the non-fluorescing components which
73 would then complement existing fluorescence EEM based measurements [2, 11, 19, 21, 22].

74 Here we show how SERS in combination with chemometric methods can be used to
75 rapidly identify and monitor chemical changes in cell culture media under different storage
76 conditions. However SERS is fundamentally difficult to implement reproducibly and thus
77 careful experimental design and a high degree of care was required during the experimental
78 work to ensure that the SERS data was both correct and reproducible. It was for this reason
79 that a silver colloid SERS substrate was used, and additionally because it avoided
80 carbonization problems that can be an issue with solid substrates. This method provided a
81 rapid, simple, and inexpensive approach for media monitoring over extended timeframes,
82 which should be of benefit for industrial biotechnology.

83

84 **2. Materials and methods**

85

86 2.1 *Materials*: eRDF was obtained from Kyokuto Pharmaceuticals Industrial (Japan).
87 Sodium bicarbonate (>99.7 %), silver nitrate (99.999 % metal basis), sodium citrate (>99.0
88 %) were obtained from Sigma-Aldrich and used without further purification. eRDF stock
89 solution (17.7 g L^{-1}) was prepared by dissolving 4.4248 g of eRDF powder and 0.2832 g of
90 sodium bicarbonate in 250 cm^3 of sterilized high purity water. The solution was immediately
91 sterilized by membrane ($0.22 \mu\text{m}$) filtration and then dispensed (1.25 mL aliquots) into sterile
92 2 mL translucent polypropylene eppendorf tubes before being placed in one of the four
93 storage conditions: 1). RT-L: Room temperature ($16.4 \pm 3.0 \text{ }^\circ\text{C}$) in the light; 2). RT-D:
94 Room temperature in the dark; 3). C-L: Cold (Fridge, $6.0 \pm 1.5 \text{ }^\circ\text{C}$) with light, and 4). C-D:
95 Cold (Fridge) in the dark. All other details have been communicated previously [11]. SERS
96 data were collected over 32 days (Day 0, 7, 11, 14, 18, 21, 25, 28, and 32). At every
97 sampling point three samples were removed from each storage condition and immediately
98 placed in the dark at 4°C to limit any further change in the samples during data acquisition.

99

100 2.2 *SERS, Raman Instrumentation, and data collection*: Silver colloid was carefully prepared
101 using the Lee and Meisel method [10, 18]. Prior to preparation all glassware was thoroughly
102 washed firstly with soap, rinsed with high purity water (HPW) from a Milli-Q® system, then
103 isopropanol, HPW, and then soaked overnight in *aqua regia* before being rinsed again with
104 HPW, until the pH of the rinsing water was neutral (pH paper). If multiple batches of colloid
105 were being prepared over a week, the glassware was only rinsed with HPW between batches.
106 Batches produced straight after cleaning of the glassware with *aqua regia* were
107 systematically discarded as they had a wider particle size distribution and larger mean size.
108 This effect was probably due to glass surface modification during cleaning, which changed
109 the dynamics of nanoparticle formation. Subsequent batches made in the same glassware
110 immediately afterwards, without cleaning, showed more consistent physical and SERS
111 properties.

112 A silver nitrate solution was first prepared by dissolving 45 mg of AgNO_3 in 250 mL of HPW
113 and brought to the boil. When the temperature of the paraffin bath reached $135 \text{ }^\circ\text{C}$, 5mL of
114 1% sodium citrate (57 mg in 5mL HPW) was slowly (~ 1 drop every 4s) introduced to the
115 boiling solution using a pressure equalizing dropping funnel. The reflux was maintained for
116 1 hour and the system was protected from the light at all times using aluminum foil. In
117 practice, a color change, from clear and colorless to opaque olive/grey, rapidly after the start
118 of the citrate addition indicates a successful preparation (absorbance maximum around 404
119 nm and full width half maximum of the absorbance $< 100 \text{ nm}$, see below).

120 UV-vis spectroscopy was used as the primary quality assurance tool as both the maximum of
121 the Plasmon resonance and the FWHM of the absorption band are symptomatic of both
122 nanoparticle size and distribution [23, 24]. Ideally, these measurements should be validated
123 using particle size measurements at the same time, but this was not available in this instance.
124 There are several published studies correlating both size and size-distribution with the UV-vis
125 spectroscopic studies, both experimentally and from a theoretical standpoint.

126 Using this approach, reasonably reproducible colloid quality was achieved with an average
127 absorbance maximum (λ_{max}) and full width half maximum (FWHM) of $404 \pm 2.5 \text{ nm}$ and
128 $86 \pm 15 \text{ nm}$ respectively (for the six batches used in this study). Batches 7 and 8 were

129 combined for this study, and this mixture was characterised by a FWHM = 86 nm and a λ_{\max}
130 (abs.) = 404 nm, which suggests an average particle size of ~20 nm [24-26]. While, the
131 particle size is smaller than the 50 nm optimum for 785 nm excitation (in terms of SERS
132 enhancement) as determined by Stamplecoskie *et al.* [26], it was appropriate for this
133 application where signal reproducibility rather than enhancement factor was the critical issue.
134 The only change observed between follow-on batches was a varying baseline in the Raman
135 spectra of the pure colloid probably due to small changes in the particle size distribution (*see*
136 *supplemental information, SI*). Finally, each colloid batch was contamination checked by
137 Raman analysis immediately prior to use.

138 SERS spectra were collected with 785 nm excitation (1 sec. exposure, 8 cm⁻¹ resolution)
139 using a RamanStation spectrometer (AVALON Instruments Ltd., Belfast) on 100 μ L sample
140 volumes in a stainless steel wellplate [14]. The effect of sample to colloid ratio (SC ratio)
141 and incubation time on the quality of the SERS spectra were investigated (*data not shown*,
142 [10]). Ultimately, a 1:19 SC ratio was selected (*vide infra*) and every test sample consisted of
143 5 μ L media solution to which was added 95 μ L of silver colloid, which was then
144 mechanically mixed using a micro-pipette. Each sample was measured immediately after
145 mixing using the super macro point mode which involved the collection of seven Raman
146 spectra (and backgrounds) from around the well center. Spectra were then co-added and each
147 sample was measured in triplicate using fresh aliquots in different wells.

148
149 **2.3 Chemometrics and data analysis:** All calculations were performed using PLS_Toolbox
150 4.0[®], supplemented by in-house-written codes for Matlab[®] (ver. 7.4). Random spikes caused
151 by cosmic rays were removed using an in-house written Matlab function. For the ageing
152 experiment, any data containing cosmic spikes were immediately recollected. Classical
153 principal component analysis (PCA) was carried out on SERS data that was baseline
154 corrected (weighted least square algorithm) and normalized (unit area).

155

156 **3. Results and discussion.**

157 One of the most critical aspects in the development of a SERS based method for complex
158 mixtures was to produce a robust sample handling procedure that delivers both signal
159 reproducibility in terms of spectral profile and intensity, and a useful SERS enhancement
160 with good signal-to-noise. We selected citrate reduced silver colloid [18] as this offers a
161 good balance between ease of preparation and effective SERS response. The quality of the
162 synthesized colloid was assessed by UV-vis spectroscopy in terms of Plasmon resonance
163 band maximum and FWHM, which serves as an excellent diagnostic tool in lieu of measuring
164 particle size distributions (*see supplemental information* and [24]). Once made these colloids
165 were carefully stored in brown glass, acid washed bottles away from any direct source of
166 light and used within 6 months of preparation. While these batches of citrate reduced colloid
167 were suitable (as evidenced in the control sample measurements, *vide infra*) for this proof-of-
168 concept study, we do recognize that the colloid batch reproducibility does not match the
169 reproducibility achieved by silver colloids generated by the reduction of hydroxylamine
170 phosphate [27]. Here to minimize the impact of colloid variation, unless stated otherwise,
171 only one batch per experiment was used.

172 However, as important as the synthesis/storage controls, the key factors affecting the
173 quality of the SERS spectra and data involved careful consideration/management of the
174 sample-colloid mixture preparation step. To avoid reproducibility and background signal
175 issues [24], we used the colloid as a suspension. Aggregation was not an issue as the eRDF
176 formulation (17.7 g L⁻¹ soln.) contained high concentrations of aggregating agents like
177 MgSO₄ (435 μM) and NaCl (105 mM). For complex media mixtures, the probability of
178 different adsorption rates, affinities, and surface coverage for the different components was
179 high and therefore one needed to carefully consider both the incubation time and sample-to-
180 colloid (SC) ratio. In addition one had to account for colloid aggregation rate, which was
181 modulated by some media components and, the time-dependent precipitation of large
182 aggregates out of solution. The first factor increased SERS signal intensity, whereas the
183 second reduced signal intensity.

184 *3.1 Spectral analysis:* Figure 1(top) shows the conventional Raman and SERS spectra of an
185 eRDF solution (17.7 g L⁻¹) and as expected the classical Raman spectra gave a very weak
186 signal that was not very diagnostic [15]. SERS in contrast gave strong signals with multiple
187 enhanced bands in the fingerprint region. Since eRDF was a complex mixture we get
188 enhancement of multiple surface adsorbed species leading to this complex signal. The
189 complexity of eRDF (with many SERS active compounds present), coupled with the different
190 enhancement factors for each analyte made an accurate assignment of each band to a
191 particular vibrational mode of a specific compound a challenging task (see *supplemental*
192 *information* for more details). We suggest that, due to their structure and relatively high
193 concentrations, most of the strong SERS signals originate from the amino acids [28-30] and
194 vitamins present. The 1394 cm⁻¹ band was probably the amino acid –COO⁻ symmetric
195 stretch [31, 32], the ~914 cm⁻¹ band the C–COO⁻ stretch, the weak band at 722 cm⁻¹ could be
196 COO⁻ deformation while the shoulder at 626 cm⁻¹ was probably due to COO⁻ wag [32]. The
197 C–S stretching of cysteine (present at 600 μM) was probably responsible for part of the 658
198 cm⁻¹ band [33], however, it was also possible that folic acid (present at 19.94 μM) also
199 contributed to this band and to the peak at 962 cm⁻¹.¹ The broad band around 1600 cm⁻¹ was
200 the water O–H bending mode with contributions from other modes such as ring CC stretches
201 of aromatic amino acids. The shape of this band in particular varies significantly (*vide infra*)
202 according to the SC ratio employed. In the context of media change identification, it was less
203 important to identify the specific source of each band, than to observe composition change.
204 The identification of the specific species involved in media change would be better suited to
205 high-resolution mass spectrometry methods.

206 *3.2 Time dependence of SERS measurements:* It has been shown [19, 34] that the incubation
207 time² can influence the profile and quality of SERS spectra. To assess the effect of different
208 incubation times on the SERS measurement of the eRDF solution, a series of SERS spectra
209 were collected over a 20 min incubation period using an arbitrarily chosen 1:4 SC ratio
210 (Figure 1). This showed that the main variation observed in the SERS spectra were increases
211 in baseline intensity and enhancement with time (Figure 2a/b). The largest increase occurred

¹ No specific vibrational mode was associated with these bands in the literature.

² Time between the moment when the sample is added to the colloid and time of the measurement.

212 during the first ~ 6 minutes, after which it slowed. The eRDF induced aggregation of the
213 nanosized Ag colloid particles, caused at first a relatively large increase in average particle
214 size, leading to very significant increase in the amount of Tyndall scattering from the sample,
215 and thus an increased baseline. After this initial growth phase, the relative increase of
216 aggregate size was much less and there were comparatively fewer particles present and thus
217 the rate of increase in Tyndall scattering decreased.

218 When the changes in the intensity of the SERS signal due to analytes were
219 investigated by plotting the integrated area of the baseline corrected spectra versus incubation
220 time (Figure 2b), it was clear that the SERS enhancement followed the same trend as the
221 baseline signal which indicated that the effects were related. This can be attributed to two
222 factors: 1). as the colloidal particles aggregate, highly angled, contact junctions between
223 particles were formed and these are known to generate dramatically larger SERS signals, and
224 2). the increased aggregate size resulted in a red-shift of the Plasmon resonance closer to the
225 excitation wavelength which further increased SERS enhancement [35].

226 The other significant aspect of the SERS spectra was the fact that the spectral profile
227 (Figure 2C) was largely unchanged over the 20 minute incubation time which indicated that
228 media components interacted very quickly with the Ag surface generating a stable population
229 of surface-bound analytes. This was supported by a PCA model of the raw SERS spectra
230 (data not shown) where only one component was needed to explain 99.85 % of the spectral
231 variance. This showed that SERS spectral changes were related only to absolute intensity
232 and not due to any changes in the surface bound population of analytes. Similarly, a single
233 component PCA model fitted using baseline corrected and normalised data explaining 99.84
234 % of the total variance. Since in both cases the explained variances were very similar and >
235 99.8 %, this meant that the difference between the spectra collected with different incubation
236 times was only a change in scale (multiplicative factor/signal enhancement increase with
237 time). However, it should be noted that the SERS spectra were only this well behaved when
238 the sample/colloid mixture was re-suspended mechanically (with a micropipette) immediately
239 prior to measurement. If this was not done, then the presence of multiple aggregating agents
240 in the eRDF caused rapid precipitation of colloid aggregates out of the suspension. When the
241 incubation experiment was implemented using different SC ratios (see *SI*) similar behaviour
242 was observed for the baseline and spectral signal intensities. However, it was also noted that
243 the spectral profile changed significantly as the SC ratio varied.

244 *3.3 Influence of SC ratio:* The profile of the SERS spectra depends dramatically (Figure 3a)
245 on SC ratio and SERS signal intensity was strongest for small SC ratios with intensity
246 gradually being decreased with additional colloid. What was more important for diagnostic
247 applications was the large spectral profile change in the normalised spectra (Figure 3b). This
248 indicated that there were very different surface analyte populations present and thus one
249 needed to exercise caution in selecting the correct ratio. For a 1:199 SC ratio, the relative
250 peak intensities were much more comparable across the spectral range which might suggest
251 that there was a much more diverse population of analytes, all of which contributed relatively
252 equally to the SERS spectrum. Since, eRDF comprised of many different molecules with
253 varying affinities for the Ag surface, the provision of excess colloid enabled more analyte
254 binding and enhancement. For example the lower affinity compounds like folic acid (bands

255 at 690, 1186, 1510, and $\sim 1595\text{ cm}^{-1}$ see *SI*) now become visible [36]. In contrast, for the
256 larger ratios (*e.g.* more sample), it was the higher affinity components (*e.g.* cysteine, C-S
257 stretch at 658 cm^{-1} [33]) that dominate the SERS spectra because they will occupy
258 proportionally more of the available sites. The variation in band intensities due to SC ratio
259 changes were not linear, for example, Figure 3c plotted the 666 cm^{-1} band intensity (which
260 probably includes the cysteine C-S stretch) against SC ratio. Band intensity first rapidly
261 increased (with a logarithmic dependence) before attaining a steady-state. It was suspected
262 that weaker bound analytes were being displaced by a smaller range of analytes which give a
263 stronger SERS response (*i.e.* those species which have a stronger affinity to the Ag surface).

264 Therefore, the SC ratio was critical for the analysis of complex media and the ratio
265 selected should be such that there were sufficient binding sites available which generated a
266 diverse and stable surface-bound population of analytes, and thus in turn led to reproducible
267 and informative SERS spectra. This must be balanced against the loss in SERS signal
268 intensity, increased background from particle scatter, and decreased signal-to-noise (S/N)
269 which is a consequence of using a small SC ratio (*e.g.* $< \sim 1:20$). The lower S/N resulted from
270 first poorer aggregation because of lower levels of intrinsic aggregating agents from the cell
271 culture media and second the lower analyte concentrations gave weaker SERS signals. One
272 way to overcome this second point would be to add a separate aggregating agent to the
273 sample/colloid mixture. However, this has to be carried out with care as this addition could
274 introduce anomalies in the SERS spectra [37]. On the basis of the experimental studies
275 (Figure 3c) we selected an SC ratio of 1:19 for the media degradation studies as this offered
276 the best compromise in terms of S/N and spectral quality.

277 *3.4 SERS monitoring of media storage induced changes:* The validity of the storage induced
278 changes as measured by SERS was confirmed by comparison (Figure 4) of test spectra
279 collected on freshly prepared eRDF solutions with the control sample (stored for 32 days at –
280 $70\text{ }^{\circ}\text{C}$) spectra. The plots showed that the SERS spectra did not change significantly (*e.g.* due
281 to different colloid performance, instrument settings) over the 32 day period of the
282 experiment. There was a small decrease in intensity for two peaks observed and this might
283 be attributable to some variance induced during the freeze-thaw cycle. However, these were
284 very small when compared to the differences observed due to the different storage conditions.

285 It was clear from the eRDF SERS spectra from the different storage conditions
286 (Figure 5) that light exposure caused a great degree of spectral change. The largest light-
287 induced change were manifested as an increased background which originated from
288 riboflavin photo-products and its associated photosensitized degradation of other components
289 [3-5, 7, 8, 10]. This resulted in changes in riboflavin and tryptophan, concentrations with the
290 simultaneous formation of lumichrome [8, 11]. One potential source of baseline signal was
291 the formation of a citrate-lumichrome complex [38], which has red fluorescence emission.
292 The colloid used here had a significant citrate concentration (both surface bound and free in
293 solution) which could bind to lumichrome, generating the red emitting fluorophore. A
294 secondary source of background was variable aggregation dynamics caused by the changed
295 chemical composition.

296 What was more interesting was the very significant changes in SERS signal for the
297 samples dark-stored where there was no photo-degradation as shown by EEM fluorescence

298 analysis which showed virtually no change ([10, 11]). Since the control experiment (Figure
299 4) showed minimal SERS spectral change for samples stored at $-70\text{ }^{\circ}\text{C}$, the obvious
300 conclusion was that solution phase chemical reactions between media components had
301 occurred. These changes in dark-stored media occurred in two principal regions: a loss of
302 signal intensity in the $660\text{-}680\text{ cm}^{-1}$ band and the appearance of two new bands in the 1520-
303 1760 cm^{-1} region. The interpretation of these spectral changes in terms of specific chemical
304 constituents was not possible with a high degree of certainty because of the sample
305 complexity and because of the convoluted interplay between selective enhancements,
306 aggregation rates etc. In addition the presence of high aggregating agent concentrations (*e.g.*
307 KCl, NaCl, MgSO_4 , *etc.*) in the eRDF made definitive band assignment more problematical
308 as it is well known that the SERS behaviour of some amino acids like cysteine can be
309 strongly influenced by the aggregating agent [37]. However, cysteine which was present at
310 relatively high concentration was easily oxidised to cystine in solution, particularly in the
311 presence of ferric [39] or cupric ions (both present in eRDF). Furthermore, the SERS
312 behaviour of cysteine/cystine shows good correlation with the changes observed here (*vide*
313 *infra*) [28, 33, 37, 40-42]. To validate these observations we attempted to measure the
314 cysteine concentration changes using chromatographic means [43, 44]. However, the
315 separation of cysteine/cystine was problematical and a pre-treatment step with iodoacetic acid
316 was required prior to the derivatisation step with PTC to obtain the S-carboxymethyl-
317 derivative of cysteine [45] (details in *supplemental information*). This was time-consuming
318 and in the case of the eRDF media, had a negative impact on the quality of the HPLC results.
319 Thus it was not possible to obtain accurate cysteine concentration data from our HPLC **setup**.

320 Therefore, to better understand the source of chemical change, Principal Component
321 Analysis (PCA) was then used to analyse the SERS spectral changes. The dark stored
322 samples were modelled using two components (99.77 % explained spectral variance) whereas
323 light exposed samples required three components (99.83 % explained variance). In both
324 cases (Figure 7), the first and second PCA components were very similar (see *SI*). PC1
325 scores increased with storage time while PC2 decreased (Figure 6) which suggested that these
326 components were associated with the degradation product(s) and the loss of a component
327 respectively. A possible interpretation of the variations modelled by PC1 and PC2 could be
328 the oxidation of cysteine (PC2) and possible production of cystine (PC1). When the PC1
329 and PC2 loadings were compared with published SERS data for both cystine and cysteine
330 [28, 37, 40, 46] there was good agreement. In particular, the match between all the bands in
331 PC2 and the SERS spectra of cysteine on citrate reduced silver colloids was very good [37,
332 40] (see *SI*). We note that in PC2 we did not observe any bands around 540 cm^{-1} (S-S
333 stretch) which would indicate the presence of the cystine dimer bound to the surface [46]. In
334 PC1, there was a broad band at 538 cm^{-1} which could be the $\nu(\text{S-S})$ vibrational mode as
335 suggested by recent SERS studies into the behaviour of both cysteine and cystine on Au and
336 Ag substrates [40]. The most likely explanation for these observations was that, during
337 storage the cysteine (PC2) originally present in the medium gradually oxidises to the dimer,
338 cystine (PC1). An alternative cysteine oxidative degradation pathway involving the
339 generation of sulfonic acids by more extreme oxidation was studied by SERS [42]. The
340 oxidation products (tentatively identified as sulfonic/sulfonic acids) have SERS spectra

341 similar to PC1 (see *SI*). The third possibility is that as cysteine is removed by oxidation,
342 binding sites on the colloid are freed up thus enabling other media components with poorer
343 affinity for the colloid to adsorb and generate a different SERS spectrum. However, on the
344 balance of the available evidence it is the cysteine-cystine conversion that is the most
345 probable source of the observed changes in the SERS spectra for the dark-stored samples.

346 In the case of the light exposed samples, SERS is less useful as the degradation is
347 more easily monitored using fluorescence [11]. However, it was noted that in the PCA model
348 of the light exposed samples that the first two components were very similar to those
349 obtained for the dark-stored samples. The third PC in the light exposed PCA model
350 originates from baseline effects probably induced by the photo-products (see above). It was
351 also noted from the PCA scores (Figure 6) that the rates of change were greater in the light
352 than for dark-stored media (see *SI* for 2D scores plots, Figure S-11). In addition, for the
353 light-stored samples there was no observable temperature effect (Figure 6d) on the PC2
354 scores (cysteine decrease) as was the case for the dark-stored samples (Figure 6b).

355 **4. Conclusions**

356 SERS was able to detect changes in chemically defined cell culture media which
357 occur under normal, cold, dark storage conditions. The SERS reproducibility issues was
358 overcome by the implementation of rigorous quality control in the synthesis and handling of
359 the citrate reduced Ag colloid, combined with a carefully designed sample incubation/data
360 collection protocol. With these procedures we showed that substrate induced variation was
361 much less than that caused by media ageing and thus the method was effective for media
362 change analysis. Significant changes were observed both in irradiated and non-irradiated
363 media which suggested that the phenomena observed by SERS were different to those
364 observed by multi-dimensional fluorescence measurements [11]. A key conclusion was that
365 large variations in the cell culture media chemical composition occur at an early stage with
366 dark-stored media (within the first 5 to 10 days after preparation). The data suggests strongly
367 that in the dark the most significant chemical change involved cysteine oxidation which takes
368 place rapidly over the first 15 days, after which media composition stabilises. PCA of the
369 SERS data allowed for qualitative monitoring of cysteine changes and this is useful since it is
370 known that cysteine form promotes cell growth which is not the case for cystine [47].
371 Furthermore, to the best of our knowledge, there is no other rapid and easy to implement
372 technique available for monitoring this cysteine-cystine change. HPLC required intensive
373 sample handling and preparation, and was not an easy method to implement for the
374 quantification of cysteine-cystine and thus identification of media change. In contrast, the
375 SERS technique presented here allows for rapid monitoring of the cysteine-cystine change
376 with minimal sample handling and preparation. Finally, since we need neither high
377 resolution nor sensitivity, this SERS method can be implemented using relatively low-cost
378 bench top Raman spectrometers thus reducing the overall cost of media testing.

379 **5. Acknowledgements**

380 AC acknowledges funding support from IRCSET (Irish Research Council for Science,
381 Engineering & Technology).

382 **6. Supplemental information available**

383 Supporting information is available including further details on the spectral and quantitative
384 analyses.
385
386

387 **References**

- 388 [1] F. Chua, S. Oh, M. Yap, W. Teo, Enhanced IgG production in eRDF media with and
389 without serum: A comparative study, *J Immunol Methods*, 167 (1994) 109-119.
- 390 [2] P.W. Ryan, B. Li, M. Shanahan, K.J. Leister, A.G. Ryder, Prediction of Cell Culture
391 Media Performance Using Fluorescence Spectroscopy, *Anal. Chem.*, 82 (2010) 1311-1317.
- 392 [3] R.J. Wang, J.D. Stoen, F. Landa, Lethal Effect of Near-Ultraviolet Irradiation on
393 Mammalian-Cells in Culture, *Nature*, 247 (1974) 43-45.
- 394 [4] R.J. Wang, Lethal Effect of Daylight Fluorescent Light on Human Cells in Tissue-
395 Culture Medium, *Photochem. Photobiol.*, 21 (1975) 373-375.
- 396 [5] B.T. Nixon, R.J. Wang, Formation of photoproducts lethal for human cells in culture
397 by daylight fluorescent light and bilirubin light., *Photochem. Photobiol.*, 26 (1977) 589-593.
- 398 [6] A.M. Edwards, E. Silva, B. Jofre, M.I. Becker, A.E. Deioannes, Visible-Light Effects
399 on Tumoral Cells in a Culture-Medium Enriched with Tryptophan and Riboflavin, *J.*
400 *Photochem. Photobiol. B-Biol.*, 24 (1994) 179-186.
- 401 [7] J.D. Stoen, R.J. Wang, Effect of Near-Ultraviolet and Visible Light on Mammalian-
402 Cells in Culture .2. Formation of Toxic Photoproducts in Tissue-Culture Medium by
403 Blacklight, *Proc. Natl. Acad. Sci. U. S. A.*, 71 (1974) 3961-3965.
- 404 [8] L. Zang, R. Frenkel, J. Simeone, M. Lanan, M. Byers, Y. Lyubarskaya, Metabolomics
405 Profiling of Cell Culture Media Leading to the Identification of Riboflavin Photosensitized
406 Degradation of Tryptophan Causing Slow Growth in Cell Culture, *Anal. Chem.*, 83 (2011)
407 5422-5430.
- 408 [9] Y. Jing, M. Borys, S. Nayak, S. Egan, Y.M. Qian, S.H. Pan, Z.J. Li, Identification of
409 cell culture conditions to control protein aggregation of IgG fusion proteins expressed in
410 Chinese hamster ovary cells, *Process Biochem.*, 47 (2012) 69-75.
- 411 [10] A. Calvet, Ph.D. Chemistry, National University of Ireland Galway, Galway, 2012, p.
412 269.
- 413 [11] A. Calvet, B. Li, A.G. Ryder, A rapid fluorescence based method for the quantitative
414 analysis of cell culture media photo-degradation, *Anal. Chim. Acta*, 807 (2014) 111-119.
- 415 [12] R. Bro, PARAFAC. Tutorial and applications, *Chemometr. Intell. Lab. Syst.*, 38
416 (1997) 149-171.
- 417 [13] A. de Juan, R.A. Tauler, Multivariate curve resolution (MCR) from 2000: progress in
418 concepts and applications, *Crit. Rev. Anal. Chem.*, 36 (2006) 163-176.
- 419 [14] A.G. Ryder, J. De Vincentis, B.Y. Li, P.W. Ryan, N.M.S. Sirimuthu, K.J. Leister, A
420 Stainless Steel Multi-Well Plate (SS-MWP) for High-Throughput Raman Analysis of Dilute
421 Solutions, *J. Raman Spectrosc.*, 41 (2010) 1266-1275.
- 422 [15] B. Li, P.W. Ryan, B.H. Ray, K.J. Leister, N.M.S. Sirimuthu, A.G. Ryder, Rapid
423 Characterisation and Quality Control of Complex Cell Culture Media using Raman
424 Spectroscopy and Chemometrics., *Biotechnol. Bioeng.*, 107 (2010) 290-301.
- 425 [16] A.G. Ryder, Surface enhanced Raman scattering for narcotic detection and
426 applications to chemical biology, *Curr. Opin. Chem. Biol.*, 9 (2005) 489-493.
- 427 [17] K. Kneipp, J. Flemming, Surface enhanced Raman scattering (SERS) of nucleic acids
428 adsorbed on colloidal silver particles, *Journal of Molecular Structure*, 145 (1986) 173-179.

- 429 [18] P.C. Lee, D. Meisel, Adsorption and Surface-Enhanced Raman of Dyes on Silver and
430 Gold Sols, *J. Phys. Chem.*, 86 (1982) 3391-3395.
- 431 [19] B. Li, N.M.S. Sirimuthu, B.H. Ray, A.G. Ryder, Using surface enhanced Raman
432 scattering (SERS) and fluorescence spectroscopy for screening yeast extracts, a complex
433 component of cell culture media., *J. Raman Spectrosc.*, 43 (2012) 1074-1082.
- 434 [20] L. Rodriguez-Lorenzo, L. Fabris, R.A. Alvarez-Puebla, Multiplex optical sensing with
435 surface-enhanced Raman scattering: A critical review, *Anal. Chim. Acta*, 745 (2012) 10-23.
- 436 [21] B. Li, P.W. Ryan, M. Shanahan, K.J. Leister, A.G. Ryder, Fluorescence EEM
437 Spectroscopy for Rapid Identification and Quality Evaluation of Cell Culture Media
438 Components., *Appl. Spectrosc.*, 65 (2011) 1240-1249.
- 439 [22] C. Calvet, B. Li, A.G. Ryder, Rapid quantification of tryptophan and tyrosine in
440 chemically defined cell culture media using fluorescence spectroscopy., *J. Pharm. Biomed.*
441 *Anal.*, 71 (2012) 89-98.
- 442 [23] O.V. Dement'eva, V.M. Rudoy, Colloidal synthesis of new silver-based
443 nanostructures with tailored localized surface plasmon resonance, *Colloid J.*, 73 (2011) 724-
444 742.
- 445 [24] I.A. Larmour, K. Faulds, D. Graham, SERS activity and stability of the most
446 frequently used silver colloids, *J. Raman Spectrosc.*, 43 (2012) 202-206.
- 447 [25] N.L. Sukhov, N.B. Ershov, V.K. Mikhalko, A.V. Gordeev, Absorption spectra of
448 large colloidal silver particles in aqueous solution, *Russ. Chem. Bull. (Transl. of Izv. Akad.*
449 *Nauk, Ser. Khim.)*, 46 (1997) 197-199.
- 450 [26] K.G. Stamplecoskie, J.C. Scaiano, V.S. Tiwari, H. Anis, Optimal Size of Silver
451 Nanoparticles for Surface-Enhanced Raman Spectroscopy, *J. Phys. Chem. C*, 115 (2011)
452 1403-1409.
- 453 [27] P. White, J. Hjortkjaer, Preparation and characterisation of a stable silver colloid for
454 SER(R)S spectroscopy, *J. Raman Spectrosc.*, 45 (2014) 32-40.
- 455 [28] E. Podstawka, Y. Ozaki, L.M. Proniewicz, Part I: Surface-enhanced Raman
456 spectroscopy investigation of amino acids and their homodipeptides adsorbed on colloidal
457 silver, *Appl. Spectrosc.*, 58 (2004) 570-580.
- 458 [29] K. Sang Kyu, K. Myung Soo, S. Se Won, Surface-enhanced Raman scattering (SERS)
459 of aromatic amino acids and their glycyl dipeptides in silver sol, *J. Raman Spectrosc.*, 18
460 (1987) 171-175.
- 461 [30] E. Podstawka, Y. Ozaki, L.M. Proniewicz, Adsorption of S-S containing proteins on a
462 colloidal silver surface studied by surface-enhanced Raman spectroscopy, *Appl. Spectrosc.*,
463 58 (2004) 1147-1156.
- 464 [31] G.D. Fleming, J.J. Finnerty, M. Campos-Vallette, F. Celis, A.E. Aliaga, C. Fredes, R.
465 Koch, Experimental and theoretical Raman and surface-enhanced Raman scattering study of
466 cysteine, *J. Raman Spectrosc.*, 40 (2009) 632-638.
- 467 [32] S. Stewart, P.M. Fredericks, Surface-enhanced Raman spectroscopy of amino acids
468 adsorbed on an electrochemically prepared silver surface, *Spectrochim. Acta, Part A*, 55A
469 (1999) 1641-1660.

- 470 [33] C.Y. Jing, Y. Fang, Experimental (SERS) and theoretical (DFT) studies on the
471 adsorption behaviors of L-cysteine on gold/silver nanoparticles, *Chem. Phys.*, 332 (2007) 27-
472 32.
- 473 [34] Y. Chen, L. Wu, Y. Chen, N. Bi, X. Zheng, H. Qi, M. Qin, X. Liao, H. Zhang, Y.
474 Tian, Determination of mercury(II) by surface-enhanced Raman scattering spectroscopy
475 based on thiol-functionalized silver nanoparticles, *Microchim. Acta*, 177 (2012) 341-348.
- 476 [35] E.C. Le Ru, E. Blackie, M. Meyer, P.G. Etchegoin, Surface enhanced Raman
477 scattering enhancement factors: a comprehensive study, *J. Phys. Chem. C*, 111 (2007) 13794-
478 13803.
- 479 [36] R.J. Stokes, E. McBride, C.G. Wilson, J.M. Girkin, W.E. Smith, D. Graham, Surface-
480 enhanced Raman scattering spectroscopy as a sensitive and selective technique for the
481 detection of folic acid in water and human serum, *Appl. Spectrosc.*, 62 (2008) 371-376.
- 482 [37] N.R. Yaffe, E.W. Blanch, Effects and anomalies that can occur in SERS spectra of
483 biological molecules when using a wide range of aggregating agents for hydroxylamine-
484 reduced and citrate-reduced silver colloids, *Vibrational Spectroscopy*, 48 (2008) 196-201.
- 485 [38] Z. Miskolczy, L. Biczok, Anion-induced changes in the absorption and fluorescence
486 properties of lumichrome: A new off-the-shelf fluorescent probe, *Chem. Phys. Lett.*, 411
487 (2005) 238-242.
- 488 [39] R.F. Jameson, W. Linert, A. Tschinkowitz, Anaerobic Oxidation of Cysteine to
489 Cystine by Iron(III) .2. The Reaction in Basic Solution, *J. Chem. Soc.-Dalton Trans.* (1988)
490 2109-2112.
- 491 [40] E. Lopez-Tobar, B. Hernandez, M. Ghomi, S. Sanchez-Cortes, Stability of the
492 Disulfide Bond in Cystine Adsorbed on Silver and Gold Nanoparticles As Evidenced by
493 SERS Data, *J. Phys. Chem. C*, 117 (2013) 1531-1537.
- 494 [41] A.G. Brolo, P. Germain, G. Hager, Investigation of the adsorption of L-cysteine on a
495 polycrystalline silver electrode by surface-enhanced Raman scattering (SERS) and surface-
496 enhanced second harmonic generation (SESHG), *J. Phys. Chem. B*, 106 (2002) 5982-5987.
- 497 [42] C.V. Stevani, D.L.A. de Faria, J.S. Porto, D.J. Trindade, E.J.H. Bechara, Mechanism
498 of automotive clearcoat damage by dragonfly eggs investigated by surface enhanced Raman
499 scattering, *Polym. Degrad. Stabil.*, 68 (2000) 61-66.
- 500 [43] V.P. Hanko, J.S. Rohrer, Determination of amino acids in cell culture and
501 fermentation broth media using anion-exchange chromatography with integrated pulsed
502 amperometric detection, *Analytical biochemistry*, 324 (2004) 29-38.
- 503 [44] J.A. White, R.J. Hart, J.C. Fry, An Evaluation of the Waters PICO-TAG System for
504 the Amino-Acid-Analysis of Food Materials, *J. Autom. Chem.*, 8 (1986) 170-177.
- 505 [45] L. Campanella, G. Crescentini, P. Avino, Simultaneous determination of cysteine,
506 cystine and 18 other amino acids in various matrices by high-performance liquid
507 chromatography, *J. Chromatogr. A*, 833 (1999) 137-145.
- 508 [46] G. Diaz Fleming, J.J. Finnerty, M. Campos - Vallette, F. Célis, A.E. Aliaga, C.
509 Fredes, R. Koch, Experimental and theoretical Raman and surface - enhanced Raman
510 scattering study of cysteine, *J. Raman Spectrosc.*, 40 (2009) 632-638.

511 [47] M.W. Glacken, E. Adema, A.J. Sinskey, Mathematical descriptions of hybridoma
512 culture kinetics: II. The relationship between thiol chemistry and the degradation of serum
513 activity, *Biotechnol. Bioeng.*, 33 (1989) 440-450.

514

515

516 **List of Figures & Legends.**

517

518 **Figure 1:** (top) Raw Raman spectra of *a*) milli-Q® water, *b*) a 17.7 g/L eRDF solution, and
519 *c*). raw SERS spectrum of a 17.7 g/L eRDF solution with an SC ratio of 1:19. All three
520 spectra were collected using identical collection conditions; (bottom) Plot of raw SERS
521 spectra collected every minute (for 20 minutes) after mixing from samples with a SC ratio of
522 1:4 (see text). The sample-colloid mixture was re-suspended between each measurement and
523 the average spectra of three replicates are plotted.

524

525 **Figure 2:** Change in the SERS spectra of a 17.7 g/L solution eRDF with incubation time.
526 (a) Change in the baseline intensity of SERS spectra (average of the data points between
527 1802 and 2002 cm^{-1}); (b) Change in the integrated spectral area (250 to 2714 cm^{-1}) of the
528 baseline corrected spectra. Data shown is for three replicate measurements; (c) Plot of the
529 overlaid baselined corrected and normalised SERS spectra of all 60 spectra. The SERS were
530 spectra collected every minute after incubation for up to 20 minutes on samples with an SC
531 ratio of 1:4. The sample-colloid mixture was re-suspended between each measurement.

532

533 **Figure 3:** Baseline corrected (a), and baseline corrected and normalised to unit area (b)
534 SERS spectra of eRDF (17.7 g/L) samples with 1:1 (black, batch 1 colloid), 1:9 (grey, batch
535 3/4 colloid) and 1:199 (grey, batch 2 colloid), ratio (v/v) of sample to colloid; (c) SERS
536 intensity of the 666 cm^{-1} peak plotted against SC ratio. The line shows the logarithmic fit: y
537 $= 3168.2 \times \log(x) + 16663$, $R^2 = 0.981$. The small deviations from the log fit are probably due
538 to the use of three different colloid batches and the intrinsic synthesis variation.

539

540 **Figure 4:** Overlap of day0 (grey) and control sample (black) raw (a) and baseline corrected
541 and normalised (b) SERS spectra collected in triplicate.

542

543 **Figure 5:** Raw SERS spectra collected from eRDF solutions (17.7 g/L) stored under various
544 conditions: (a) C-D; (b) RT-D; (c) C-L, and (d) RT-L. The storage time increases from
545 black to light grey and the average spectra of three replicate are plotted.

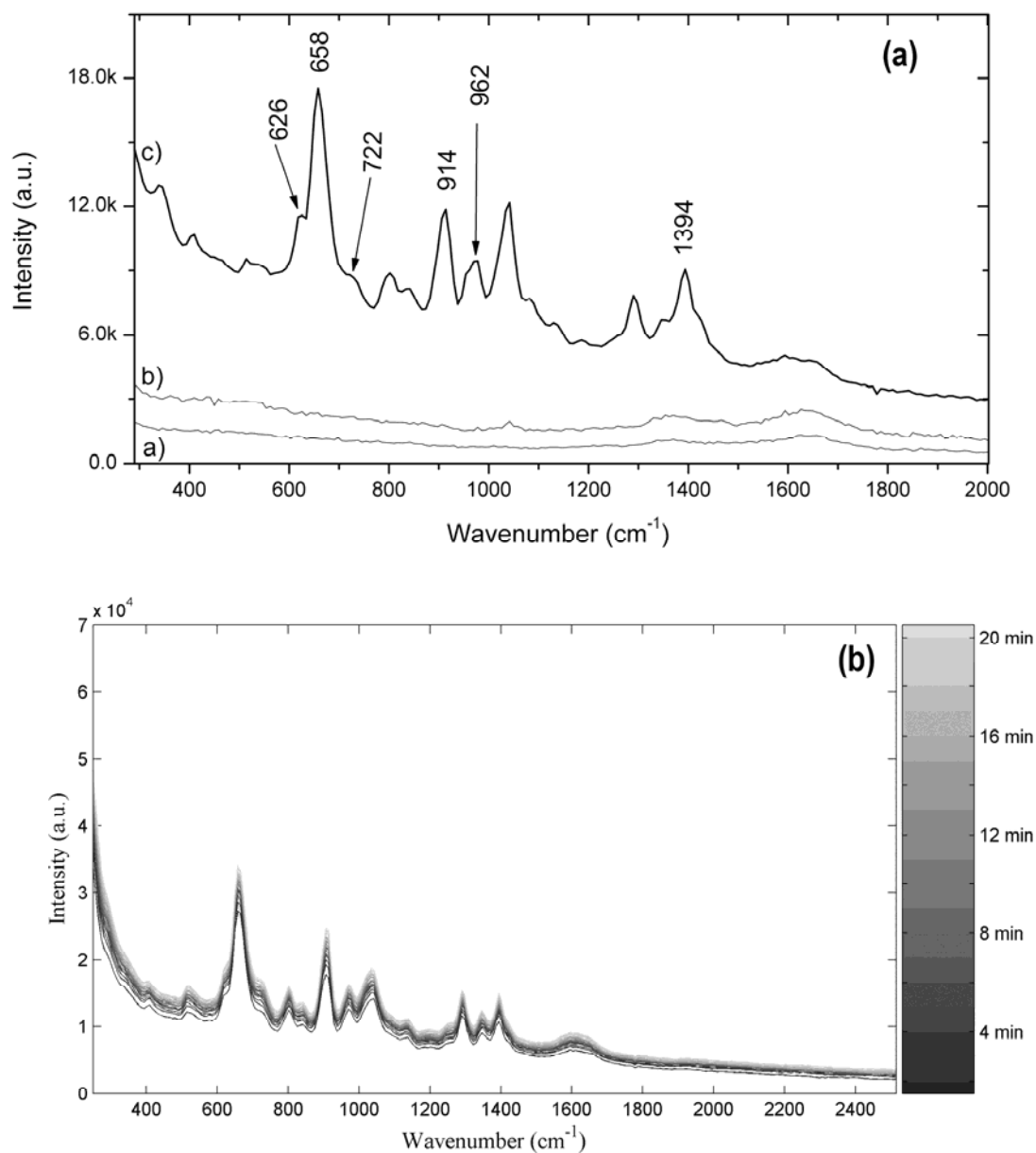
546

547 **Figure 6:** Plots of changes in the individual principal component scores versus time
548 generated by various PCA models: (a) PC1, and (b) PC2 component scores plotted versus
549 time at room temperature (\circ) and in the fridge (\square) for the dark stored samples. (c) PC1, (d)
550 PC2, and (e) PC3 component scores plotted versus time at room temperature (\circ) and in the
551 fridge (\square) for the light stored samples. PC1 vs. PC2 scores plots are available in the
552 *supplemental information*, Figure S-11.

553

554 **Figure 7:** Loadings of the components generated by the PCA analysis of the data collected
555 on the samples stored in the dark (a) and in the light (b) under both the cold and room
556 temperature storage conditions.

557
558
559



560
561
562
563
564

Figure 1.

565

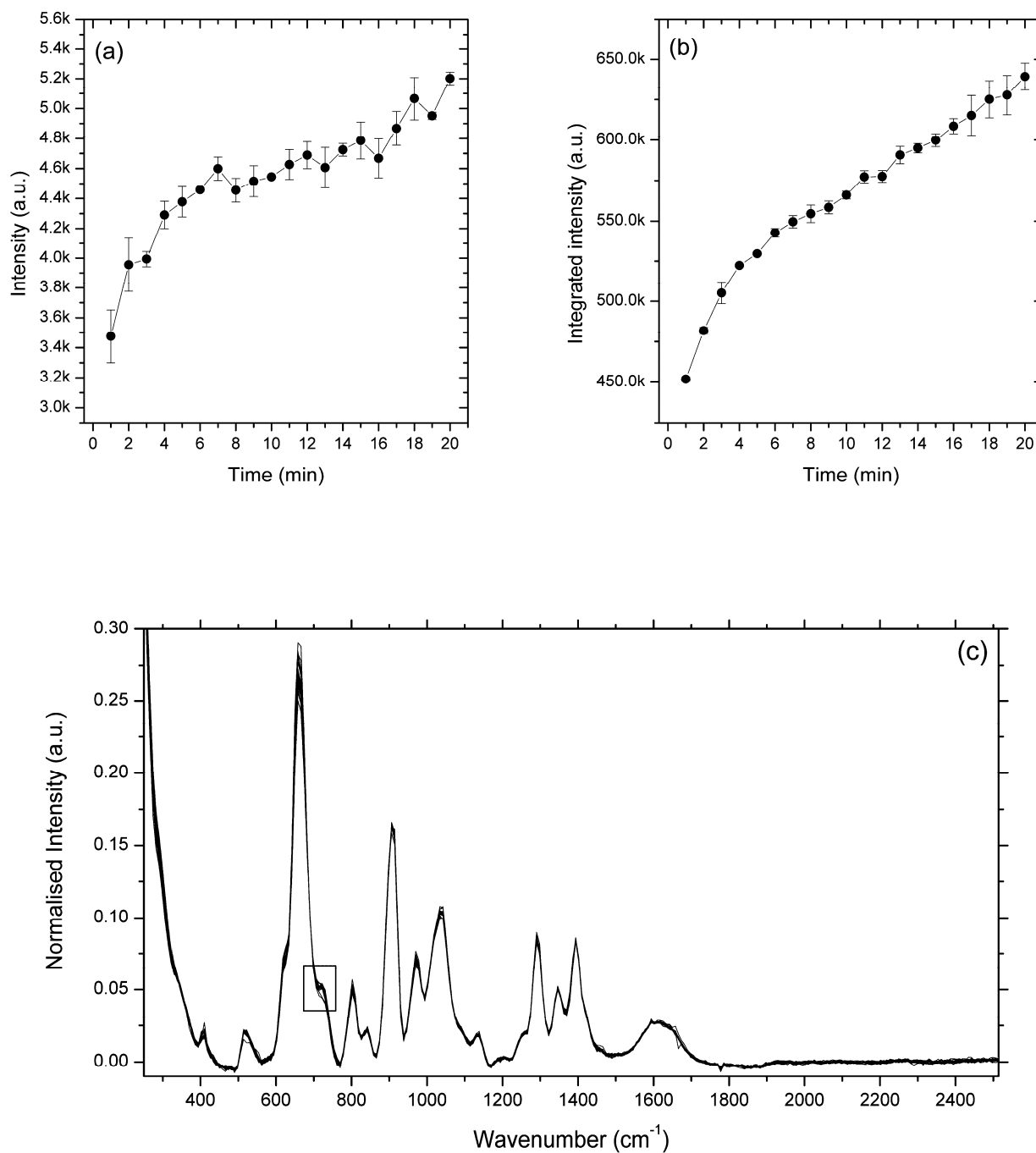
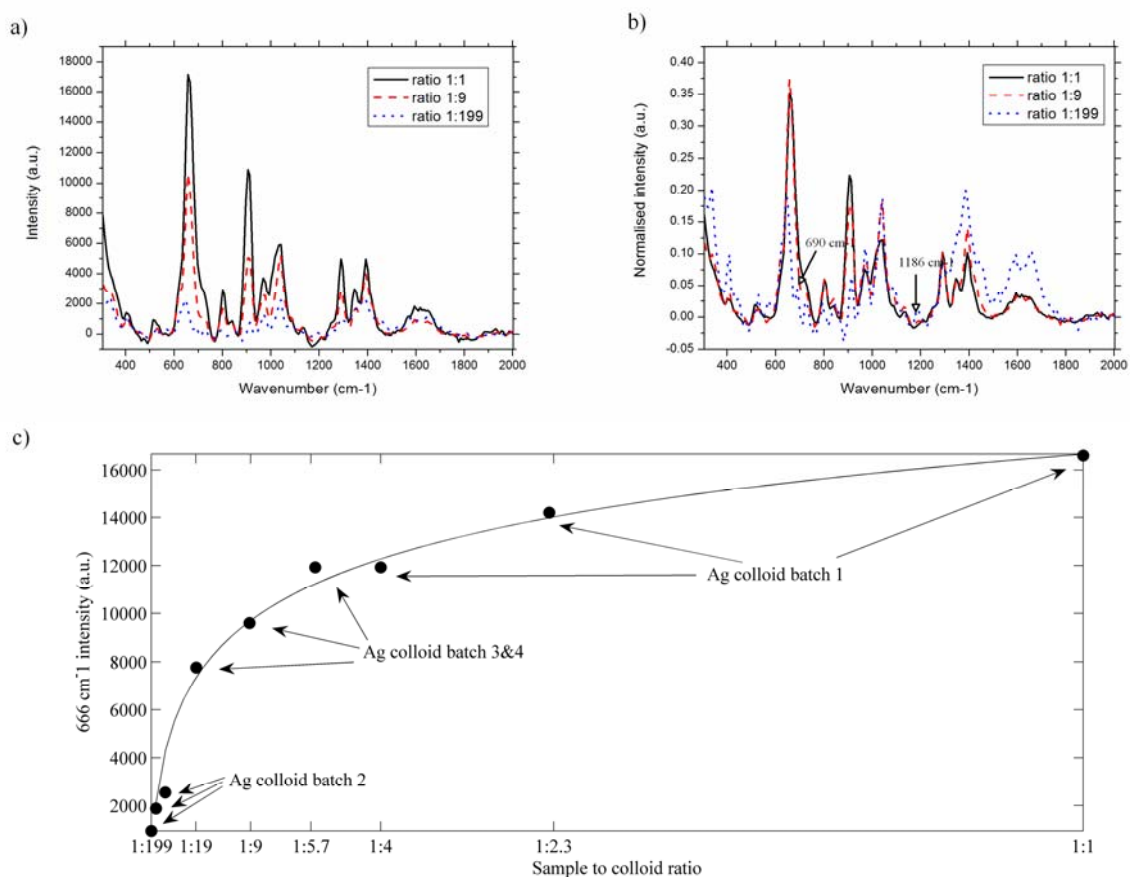


Figure 2:

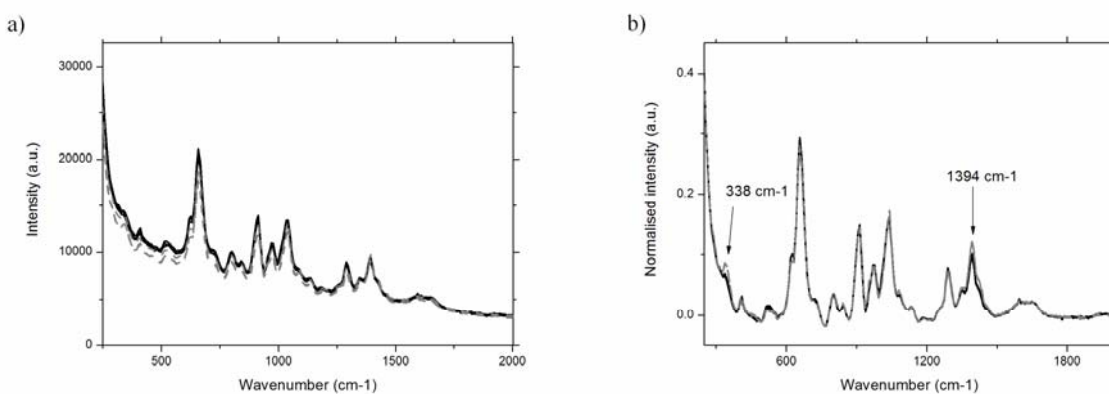
566
567
568
569

570



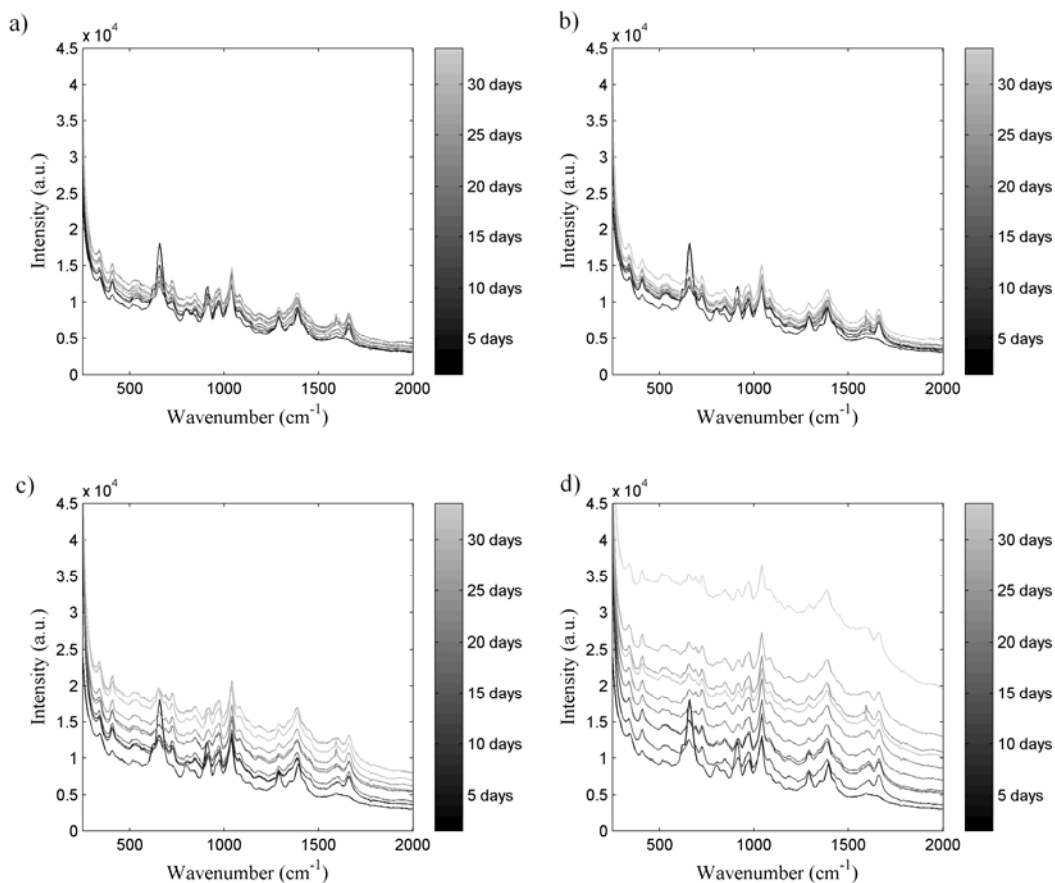
571
572
573
574

Figure 3:



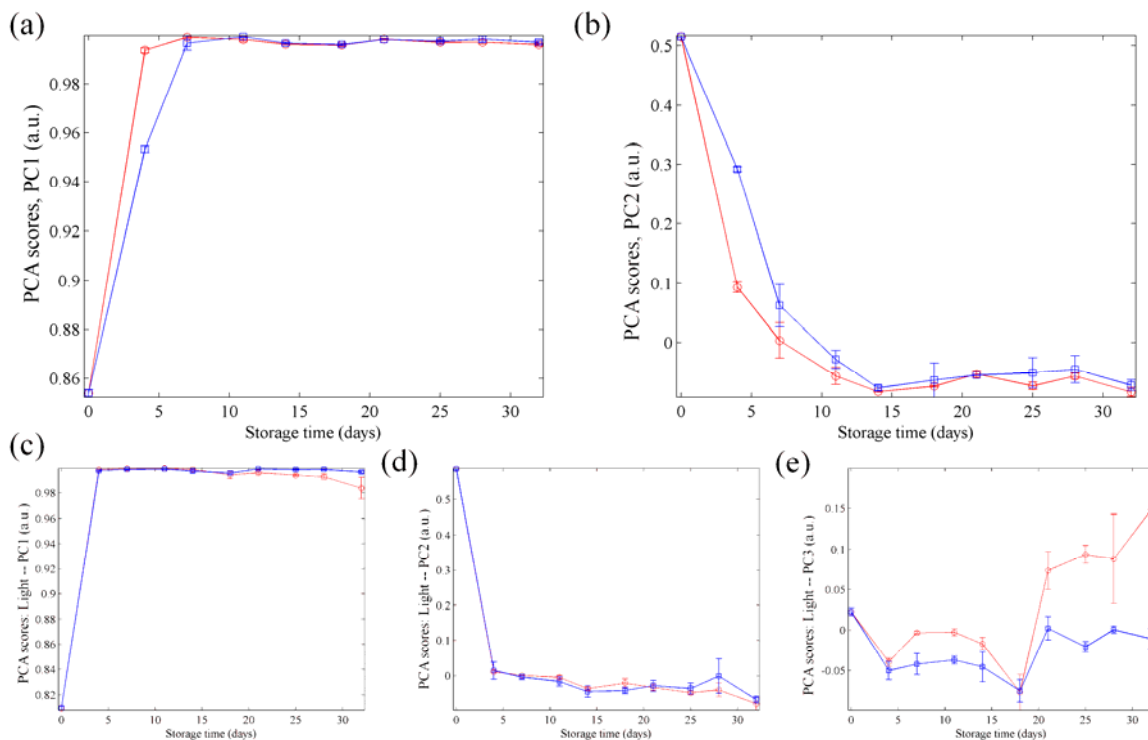
575
576
577
578
579

Figure 4:



580
581

Figure 5.



582
583

Figure 6.

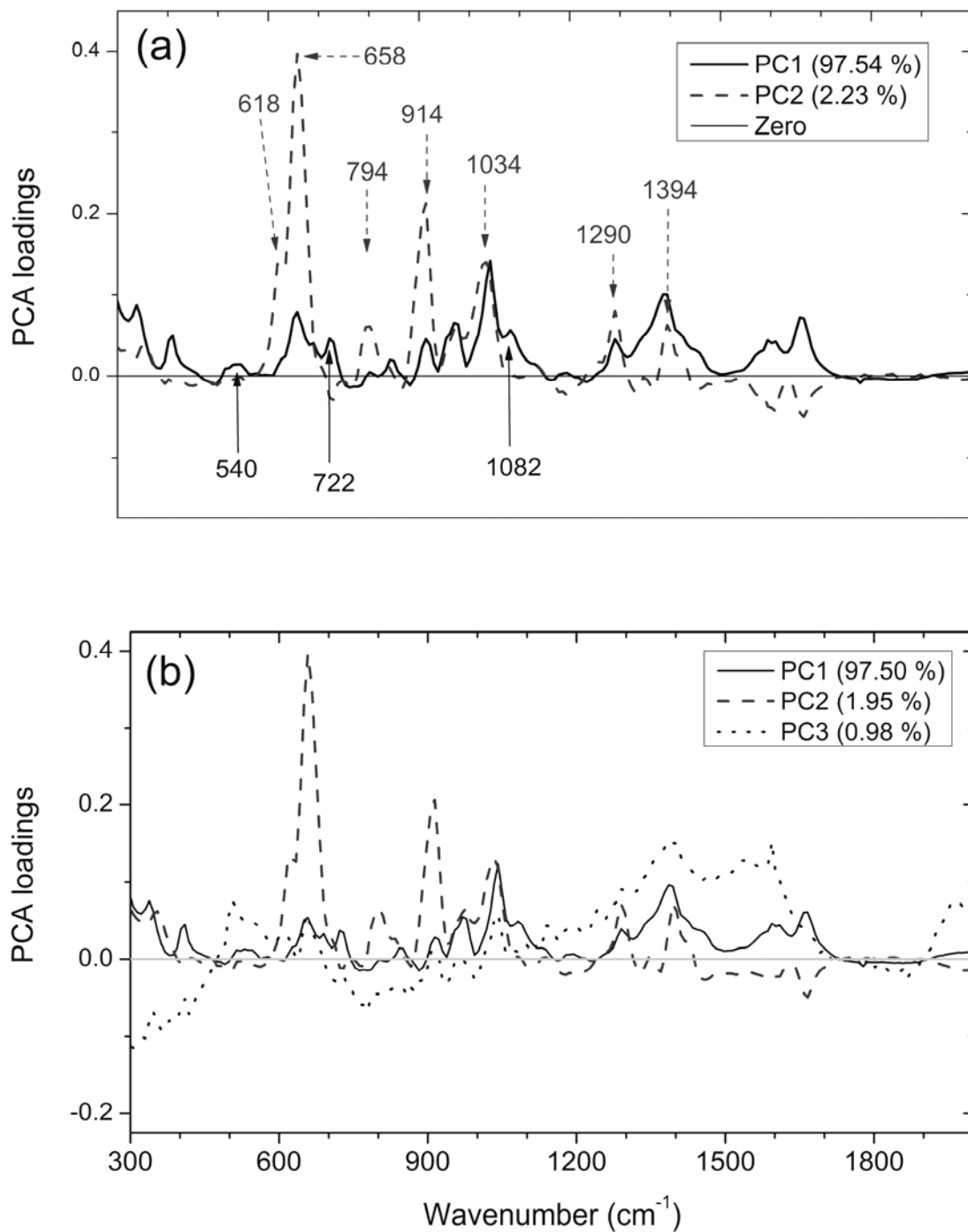


Figure 7.

584
585